

RESEARCH

Open Access



Genomic and transcriptomic landscape to decipher the genetic basis of hyperpigmentation in Lanping black-boned sheep (*Ovis aries*)

Yuqing Chong^{1†}, Heli Xiong^{1,2†}, Zhendong Gao¹, Ying Lu¹, Jieyun Hong¹, Jiao Wu¹, Xiaoming He¹, Dongmei Xi¹, Xiaolong Tu^{3,4*} and Weidong Deng^{1*}

Abstract

Background Lanping black-boned sheep (LPB) represent a distinctive mammalian species characterized by hyperpigmentation, resulting in black bone and muscle features, in contrast to their conventional counterparts exhibiting red muscle and white bone. The genetic basis underlying LPB hyperpigmentation has remained enigmatic.

Methods In this study, we conducted whole-genome sequencing of 100 LPB and 50 Lanping normal sheep (LPN), and integrated this data with 421 sequenced datasets from wild and domestic sheep, shedding light on the genetic backdrop and genomic variations associated with LPB. Furthermore, we performed comparative RNA-Seq analysis using liver sample to pinpoint genes implicated in the pigmentation process. We generated a comprehensive dataset comprising 97,944,357 SNPs from 571 sheep, facilitating an in-depth exploration of genetic factors.

Results Population genetic structure analysis revealed that the LPB breed traces its origin back to LPN, having evolved into a distinct breed. The integration of positively selected genes with differentially expressed genes identified two candidates, *ERBB4* and *ROR1*, potentially linked to LPB hyperpigmentation. Comparative analysis of *ERBB4* and *ROR1* mRNA relative expression levels in liver, spleen, and kidney tissues of LPB, in comparison to Diqing sheep, revealed significant upregulation, except for *ERBB4* in the liver. Gene expression heatmaps further underscored marked allelic frequency disparities in different populations.

Conclusion Our findings establish the evolutionary lineage of the LPB breed from LPN and underscore the involvement of *ERBB4* and *ROR1* genes in melanin synthesis. These results enhance our comprehension of the molecular basis of hyperpigmentation and contribute to a more comprehensive depiction of sheep diversity.

[†]Yuqing Chong and Heli Xiong contributed equally to this work.

*Correspondence:
Xiaolong Tu
tuxiaolong@mail.kiz.ac.cn
Weidong Deng
dengwd@ynau.edu.cn

Full list of author information is available at the end of the article



Keywords Lanping black-boned sheep (LPB), Hyperpigmentation, Whole-genome sequence, RNA-Seq, Integrative analysis

Introduction

Hyperpigmentation in animals has long piqued the curiosity of evolutionary and developmental biologists, offering valuable insights into melanocyte development and hyperpigmentation-related disease research [1–3]. Recently discovered in Lanping County, China, Lanping black-boned sheep (LPB) exhibit striking hyperpigmentation in their skin and internal tissues, resembling the world-renowned silky fowl [4]. They are unique among mammals, displaying extensive pigmentation throughout their bodies, including the eye conjunctiva, muscles, periosteum, kidney, heart, lung, liver, and trachea. This distinctive trait makes them highly prized for their superior meat quality, particularly appealing to oriental preferences. LPB are found emerging from Lanping normal sheep (LPN), which lacks hyperpigmentation in its skin and internal organs, like most sheep breeds. However, the exact genetic lineage of LPB, its relationship with LPN, and the underlying genetic mechanisms responsible for hyperpigmentation in LPB remain poorly understood.

Melanocytes and the melanin they produce play critical biological roles, including protection against UV radiation, thermal regulation, and camouflage [5]. Dysfunction of melanocytes can lead to various diseases such as albinism, melanoma, microphthalmia, and Waardenburg syndrome [6]. Melanocytes produce two types of melanin: eumelanin and pheomelanin. Melanin synthesis involves a series of complex enzymatic and biochemical reactions. The key regulatory factors in melanin production are tyrosinase (*TYR*), tyrosinase-related protein 1 (*TYRP1*), and tyrosinase-related protein 2 (*TYRP2*), with *TYR* playing a particularly crucial role. Melanin synthesis begins with the oxidation of L-tyrosine and/or L-dihydroxyphenylalanine (L-DOPA) to dopaquinone (DQ), which serves as the substrate to produce both eumelanin and pheomelanin. Dopaquinone undergoes polymerization to form colorless dopachrome. Dopachrome is highly unstable and is rapidly oxidized to dopachrome by another dopaquinone molecule. Under the action of *TYRP2*, dopachrome is hydroxylated to 5,6-dihydroxyindole-2-carboxylic acid or spontaneously decarboxylated to 5,6-dihydroxyindole. Subsequently, 5,6-dihydroxyindole is catalyzed to 5,6-indolequinone-2-carboxylic acid by *TYRP1*. 5,6-dihydroxyindole is catalyzed by *TYR* to form 5,6-indolequinone, which, along with 5,6-indolequinone-2-carboxylic acid and 5,6-indolequinone, ultimately contributes to eumelanin formation. In the presence of cysteine or other thiol-containing compounds, dopaquinone reacts with cysteine to form cysteine-dopachrome, which is further oxidized to pheomelanin. Among

these enzymatic reactions, *TYR* acts as the rate-limiting enzyme in melanin synthesis, as all other reactions can occur under physiological pH conditions [7]. The process of melanin synthesis in melanocytes is regulated by autocrine and paracrine factors. During this process, the microphthalmia-associated transcription factor (*MITF*) serves as a central regulator by upregulating the two key enzymes, *TYR* and *TYRP1*, to promote melanin production. Studies have shown that paracrine factors secreted by keratinocytes, such as *MC1R*, *EDN*, and *SCF*, are major regulators of melanin synthesis. In the skin, in addition to keratinocytes, fibroblasts and immune cells in the dermis also regulate melanin synthesis in melanocytes through paracrine factors [8]. Research on melanocytes has been continuous over the past few decades. To date, studies have primarily focused on the formation, localization, and melanin synthesis of melanocytes, as well as the key cytokines and signaling pathways involved at different stages. These investigations have progressively elucidated the molecular mechanisms underlying melanocyte development and their biological functions, providing a theoretical basis for related disease research and valuable insights for studies on economically significant traits associated with pigmentation in animals.

To date, more than 688 genes associated with pigmentation have been identified [9] (last update: 8 December 2022). These genes encompass melanocyte development-related genes such as *MITF*, *SOX10*, *PAX3*, *WNT*, *EDN3*, *EDNRB*, *KIT*, *MC1R*, and melanogenic genes including *TYR*, *TYRP1*, *DCT*, and *PEML* [6, 10]. In several studies, gene duplication of Endothelin 3 (*EDN3*) has been identified as the cause of hyperpigmentation in silky fowl [1, 3] and other black-boned chicken breeds, like the Ayam Cemani in Indonesia [11]. However, a study by Darwish et al. [12] challenged this association, revealing that *END3* duplication is not linked to hyperpigmentation in LPB. Notably, pigmentation in LPB and silky fowl followed a similar pattern of progressively darkening with age. While no pigmentation was observed at birth, it became visible at around one year of age and pronounced at approximately two years of age. Interestingly, melanin content in the liver of LPB was higher than in other tissues, including the trachea, lung, heart, kidney, and skin, but it was less pronounced and sometimes undetectable in the liver tissue of silky fowl [5, 13]. This highlights distinct mechanisms underlying hyperpigmentation in LPB compared to silky fowl. Although several pigmentation-related genes, such as *TYR* [14], *TYRP1* [15], *TYRP2* [16], and *MC1R* [17], have been explored for their potential

involvement in LPB hyperpigmentation, but no conclusive links have been established.

In this study, we aimed to provide a comprehensive understanding of the genetic phylogeny and genetic basis associated with hyperpigmentation in LPB. We achieved this by conducting whole-genome sequencing of 100 LPB and 50 LPN, followed by the integration of this data with a dataset encompassing 421 counterparts representing seven wild and 64 domestic sheep breeds from diverse geographic regions. Additionally, RNA-Seq analysis of liver tissues at two developmental stages was employed to investigate genes associated with melanocyte development and melanogenesis. Through a meticulous combination of genomic and transcriptomic analyses, we identified several potential gene implicated in hyperpigmentation.

Materials and methods

Samples collection

LPB and LPN are both local sheep breeds from Lanping County, Nujiang Prefecture, Yunnan Province, China. They share similar body size and appearance characteristics, with no apparent differences. The distinguishing feature between them lies in LPB having black trait such as black bones and black meat, while LPN lacks these traits. Both populations are raised under consistent conditions, and have no genetic relationship.

Among the 5 local sheep farms in Lanping County, a total of 100 LPB (half male and half female) with no genetic relationship, particularly obvious black-bone traits were selected from the 443 adult LPB, while 50 LPN (half male and half female) with no genetic relationship were selected from the 298 Lanping indigenous sheep. Each sheep was verified to meet the breed standards. Blood samples were drawn from the jugular vein and promptly frozen at -20°C for further analysis.

The LPB is currently the only known mammal with the black-trait, which is absent in other sheep breeds. To improve the efficiency of screening functional genes related to the black trait, we additionally included 421 sheep of diverse backgrounds. These data encompassed 37 wild sheep individuals from seven different breeds, including Mouflon, Urial, Argali, Bighorn, Thin horn, and Barbary. Furthermore, there were 384 domestic sheep samples, comprising 247 individuals from 14 different breeds in Tibet, Northern and Eastern China, and 137 individuals from 50 diverse breeds across South Asia (SA), Europe, Africa, the Middle East (ME), and Oceania. These additional samples were obtained from 227 publicly available datasets from the NCBI database and 194 datasets shared by Dr. Yu Jiang from Northwest A&F University (Supplementary table S1).

For transcriptome analysis, a total of 23 sheep were slaughtered, including 6 LPB (3 male and 3 female) and 5

LPN (2 male and 3 female) at 2 months of age, and 6 LPB (3 male and 3 female) and 6 LPN (4 male and 2 female) at about 2 years of age. Liver tissue from each individual was sampled for RNA-Seq.

Whole-genome sequence and SNPs calling

Total genomic DNA from 150 blood samples were extracted using the Takara Blood Genome DNA Extraction Kit following the manufacturer's guidelines. DNA quality and quantity was examined using a NanoDrop device and 1% agarose gel electrophoresis. Paired-end sequencing libraries were generated with an insert size of about 350 bp, according to the manufacturer's instructions, and sequenced on Illumina HiSeq X Ten platform to an average raw read sequence coverage of $\sim 10\times$. After removing the low-quality raw reads (N content ratio $> 10\%$, low quality base ratio $> 50\%$), high quality reads were mapped to the sheep reference genome assembly Oar_v4.0 using Burrows-Wheeler Aligner (BWA v0.7.15). Picard tools (v1.119) was utilized to identify and remove duplicate reads from the BAM file. After mapping, SNPs were called by GATK (v3.7.0) [18] from the BAM file and the output SNPs were further filtered using vcftools (v4.2) [19]. Raw SNPs were filtered using the following criteria, Quality Depth (QD) < 2.0 , root mean square of Mapping Quality (MQ) < 40.0 , Fisher Stand (FS) > 60.0 , HaplotypeScore > 13.0 , and MQRankSum ≤ 12.5 , and biallelic SNPs with no more than 10% missing rate. Filtered SNPs were further annotated by ANNOVAR [20] based on the gene annotation of the sheep reference genome Oar_v4.0 and then classified as variations in exonic, intronic, intergenic, upstream, downstream, 5'UTR, 3'UTR, and splicing sites.

Population Structural analysis

Principle component analysis (PCA) was performed based on autosomal SNPs for 571 individuals using GCTA (v1.92.4 beta) [21]. PLINK (v1.9) [22] was used to prune SNPs in linkage disequilibrium in a sliding 100-SNPs window at 10-SNPs steps. After pruning, 302,088 representative SNPs of 571 sheep were extracted for NJ-tree construction and structure analysis. NJ-tree was constructed based on a matrix of pairwise genetic distances using PHYLIP (v3.698) [23] and visualized using the online software iTOL (<https://itol.embl.de/>). Admixture (v1.2.3) [24] was used to assess the admixture proportions with the default setting; the number of possible genetic clusters K ranged from 2 to 8.

Introgression analysis

Based on the Patterson's D-statistic (ABBA-BABA test) [25], we used the Pythonscript ABBABABAWindows.py [26] to compute the introgression among two populations (LPB, and LPN). Windows with absolute D-statistic

values close to zero (e.g., low 1% windows) were regarded as the genomic regions least affected by gene flow, whereas the highest D-statistic values (e.g., top 1% windows) were regarded as those most affected by gene flow.

Selective sweep analysis

We calculated the genome-wide distribution of F_{ST} and $LSBL$ values between LPB and non-black-bone domestic sheep population with a 20 kb sliding window using *vcftools* (v4.2) [19], and the Cross Population Extended Haplotype Homozygosity ($XPEHH$) values were calculated using *Selscan* (v2.0.0) [27]. The top 1% of values for the F_{ST} , $LSBL$, and $XPEHH$ were considered as the candidate regions under strong selective sweeps and visualized in the R package. All the candidate regions were assigned to corresponding SNPs and genes using in-house scripts. We further performed KEGG (Kyoto Encyclopedia of Genes and Genomes) pathway and GO (Gene Ontology) terms analysis using the online software *g:Profiler* [28], and $p < 0.05$ was used as the threshold for significantly enriched pathways and GO terms [29].

RNA-Seq analysis

RNA-Seq was performed on the liver tissues of 6 LPB and 5 LPN at the pigmentation-not-visible-stage, and in 6 LPB and 6 LPN at the pigmentation-evident stage. The total RNA of 23 liver samples was isolated using Trizol RNA Reagent (Takara), according to the manufacturer's instructions. The integrity of total RNA was assessed by agarose gel (1%) electrophoresis, prepared in the same manner as for DNA detection. Electrophoresis was conducted at 100 V for 15 min. For concentration and purity analysis, 1 μ L of total RNA solution was diluted with 99 μ L of sterile water, using sterile water as a blank control. Measurements were performed using a UV-visible spectrophotometer. Then, mRNA libraries were constructed using a NEBNext Ultra Directional RNA Library Prep Kit. The mRNA libraries were then sequenced on an Illumina HiSeq X Ten platform with 100 bp paired-end reads. The raw reads were filtered by removing the low-quality reads and then mapped to the sheep reference genome *Oar_v4.0* using *TopHat* (v2.0.9) [30]. The expression abundance of each assembled transcript was measured through Fragments per Kilobase of exon model per Million mapped reads (*FPKM*) values. The *edgeR* 4.0 was used to test the significance of inter group differences in RNA-Seq data processing. The genes that exhibited $|\log_2(\text{fold change})| \geq 1$ and adjusted $p \leq 0.05$ in the comparisons between LPB and LPN individuals from two pigmentation stages were considered as differentially expressed genes (DEGs). KEGG pathway and GO term enrichment analysis of differentially expressed genes were performed using the online *OmicShare* tools.

qRT-PCR

Total RNA was isolated from liver, spleen, and kidney tissues of 6 LPB and 6 Diqing sheep individuals, utilizing Trizol reagent (Thermo Scientific). cDNA synthesis was achieved with the PrimeScript™ RT Reagent Kit with gDNA Eraser (Takara), and was synthesized by Sangon Biotech (Shanghai) Co., Ltd. Uniform cDNA concentration of 1 μ g/ μ L during reverse transcription. Quantitative RT-PCR (qRT-PCR) experiments were conducted with TB Green® Premix Ex Taq™ Takara, the cycle program of qRT-PCR consisted of pre-denaturation (95°C, 3 min), denaturation (95°C, 30 s), annealing (59°C, 30 s) and extension (72°C, 30 s), finally melt curve stage (Ramp rate: +0.5°C / 5 s). Simultaneous amplification efficiency E in the range of 90%–110%. Raw data were processed with the $\Delta\Delta C_t$ method (Kenneth & Thomas, 2001), where $\Delta C_t = C_t$ (gene of interest) – C_t (housekeeping gene); $\Delta\Delta C_t = \Delta C_t$ (treated sample) – ΔC_t (untreated sample). Primer sequence (5'-3') for the *ERBB4* gene were forward: CGGAACAGTGTGATGGCAGA, reverse: TGTG GGCACCTTCTTGACACA, and for *ROR1* gene (forward: ACAGAGTTGTCAGTCACTGCT, reverse: CTAATC CGCAGTCGAGAGCC), and reference gene is *GAPDH* (forward: GCCCTCAACGACCACTTTGT, reverse: TC GGGAGATTCTCAGTGTGG).

Results

Genome sequencing and variations

We conducted genome sequencing for a cohort of 100 LPB sheep and 50 LPN sheep (Supplementary table S1), resulting in a substantial dataset comprising 27.69 billion raw paired-end reads. This dataset yielded an average sequencing depth of 9.30X per individual, with an average genome coverage of 96.47% (Supplementary table S2). To ensure a comprehensive genomic comparison, we augmented our dataset by merging it with a larger collection of whole-genome sequences. This expanded dataset included individuals from seven wild sheep breeds ($n=37$ sheep) and 64 domestic sheep breeds ($n=384$ sheep), originating from diverse regions, including Tibet, Northern and Eastern China, South Asia, the Middle East, Africa, Europe, and Oceania [31, 32] (Supplementary table S1). The augmented dataset exhibited an average coverage depth of 9.70X per individual.

Following stringent variant filtering criteria, we identified a total of 97,944,357 high-quality single nucleotide polymorphisms (SNPs) across the entire cohort of 571 sheep (Supplementary table S3). These SNPs were categorized into various functional classes, with the majority falling into intergenic regions (65.15%) and intronic regions (32.71%) (Supplementary figure S1). Notably, LPB displayed a lower SNP density (11.81/1000 bp) and nucleotide diversity (π) (2.50×10^{-3}) in comparison to non-black-boned sheep, which encompassed LPN and

64 domestic sheep breeds (exhibiting 19.88 SNPs per 1000 bp and 2.94×10^{-3} nucleotide diversity) (Supplementary table S4).

Genetic relationship of LPB with LPN and worldwide sheep breeds

We delved into the genetic relationships of LPB with other sheep breeds in a global context. To accomplish this, we employed Principal Component Analysis (PCA) (Fig. 1A), Neighbor-Joining (NJ) phylogeny (Fig. 1B), and ADMIXTURE analysis (Fig. 1C), all of which were based on the extensive dataset of whole-genome SNPs.

The PCA plot and NJ-tree unveiled a distinct separation of Lanping local sheep, comprising both LPB and LPN, from domestic and wild sheep breeds. However, they exhibited a closer genetic affinity with Chinese sheep populations, particularly Tibetan sheep, and those from Northern and Eastern China. This observation

suggests that Lanping sheep can be regarded as a sub-population within the broader Chinese sheep genetic landscape. Tibetan sheep occupied an intermediate position between Lanping sheep and Northern and Eastern Chinese sheep, and have strong genetic affinity with the latter two. ADMIXTURE analysis further substantiated this relationship, revealing that Tibetan and Northern and Eastern Chinese sheep exhibited higher levels of shared ancestral components than they did with LPB and LPN when analyzed at $K=4$. This aligns with a prior study, which reported a closer genetic connection between Tibetan and Northern and Eastern Chinese sheep in contrast to the relationship between Tibetan sheep and Yunnan-Kweichow sheep populations [31].

The Principal Component Analysis (PCA) plot did not exhibit a clear demarcation between LPB and LPN populations. However, the Neighbor-Joining (NJ) phylogenetic tree revealed that while LPB and LPN clustered together

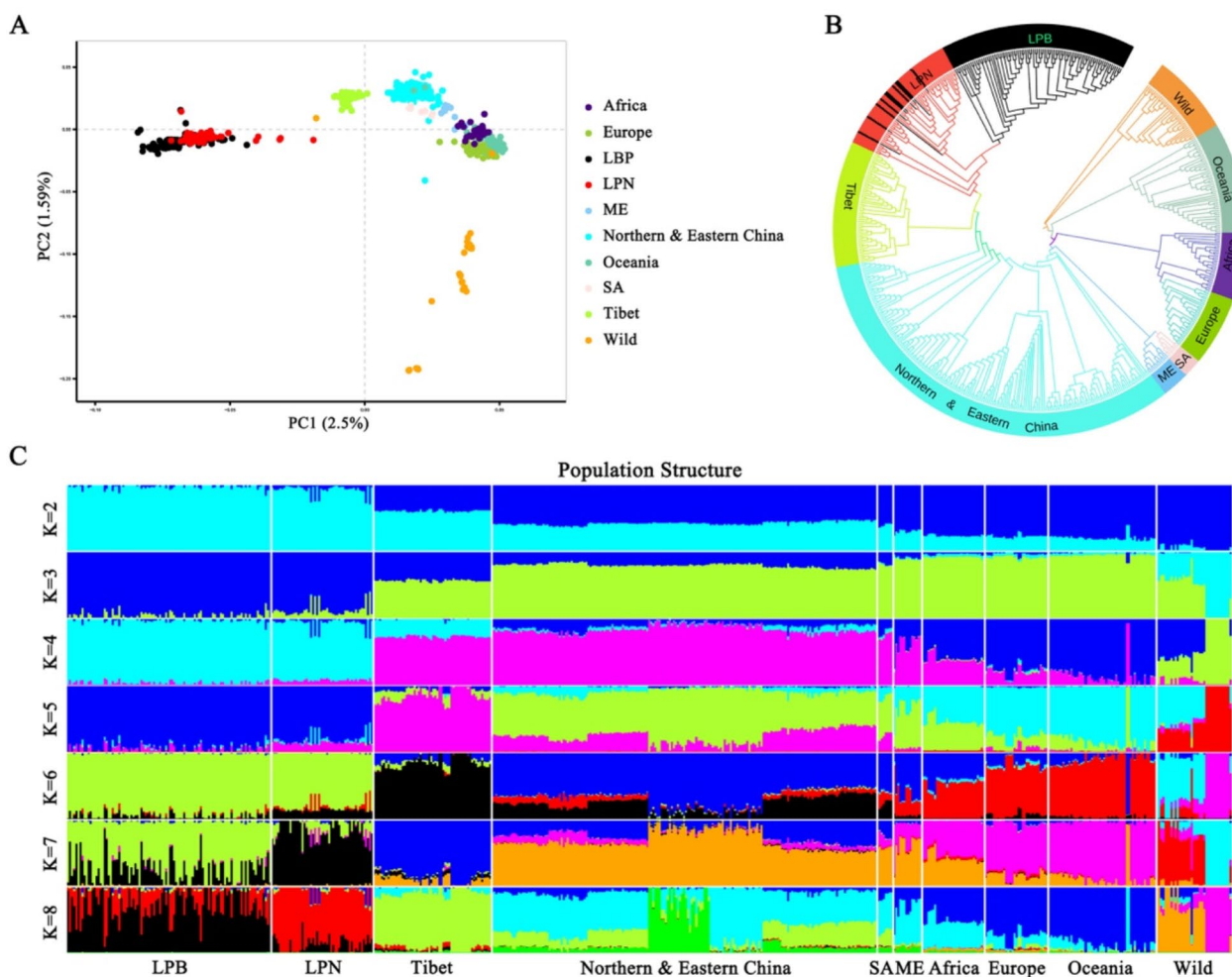


Fig. 1 Population genetic analysis of LPB and 9 subgroups of 571 domestic and wild sheep individuals from around the world. **A:** Principal components 1 and 2 for 571 individual sheep. **B:** Neighbor-joining phylogenetic tree of 571 individual sheep. **C:** Population structure of individual 571 with $K=2-8$. The abbreviations and subgroups of the breeds and individuals are shown in Supplementary table S1

in one clade, they further separated into two distinct sub-clusters. Notably, within this sub-cluster delineation, ten LPB individuals displaying hyperpigmentation traits were found to be nested within the LPN branch (Fig. 1B). This intriguing observation raises the possibility that these ten individuals may represent hybrid progeny resulting from interbreeding between LPB and LPN.

ADMIXTURE analysis also supports the results of the PCA and physiological tree mentioned above (Fig. 1C), and the admixture levels and genetic components indicated a high ancestral coefficient and a strong genetic resemblance between the two populations. Nevertheless, a more nuanced perspective emerged when assessing genetic divergence through pairwise fixation index (F_{ST}) calculations. The F_{ST} value of 0.0210 between LPB and LPN surpassed the genetic differentiation observed between three separate breeds of Tibetan lineage, with $F_{ST(TIB/OLA)}=0.0150$, $F_{ST(TIB/PRT)}=0.0184$, and $F_{ST(PRT/OLA)}=0.0154$ (Table 1). Therefore, while LPB and LPN displayed robust genetic similarities, the notable genetic divergence, as indicated by the F_{ST} value, suggests that LPB is indeed derived from LPN and has evolved into a distinct breed.

Genomic signatures associated with hyperpigmentation in LPB

To identify genomic signatures associated with hyperpigmentation in LPB, we conducted a comprehensive analysis of the genome. We assessed allele frequency differentiation by calculating F_{ST} between the LPB population and none-black-boned domestic sheep. Using a window size of 20 kb and a step size of 10 kb, we detected a total of 576 putatively positively selected genes (PSGs) based on empirical distributions (with a cutoff of the top 1st percentile) (Fig. 2, Supplementary table S5).

Gene Ontology (GO) enrichment analysis of these PSGs revealed an enrichment in processes related to development. Additionally, a significant Kyoto Encyclopedia of Genes and Genomes (KEGG) pathway, the MAPK signaling pathway, was identified, which is crucial

for melanocyte development and melanogenesis. This pathway includes 16 genes: *MAP3K1*, *ANGPT1*, *DUSP1*, *TGFB3*, *NFKB1*, *FGF7*, *ERBB4*, *KIT*, *NF1*, *MAPKAPK5*, *FGFR4*, *PTPN5*, *TP53*, *MAP3K12*, *FGFR1*, *MAP4K4* (Supplementary table S6 and S7).

Furthermore, we employed locus-specific branch length statistics (*LSBL*) to analyze the population of LPB, none black-boned sheep, and wild sheep using LPB as the target population. By applying a window size of 20 kb and a step size of 10 kb, we identified 504 genes as PSGs based on empirical distributions (with a cutoff of the top 1st percentile) (Fig. 2, Supplementary table S8). KEGG and GO terms analysis of these PSGs revealed 4 pathways and 39 terms that were over-represented (Supplementary table S9 and S10). The MAPK signaling pathway, which includes 14 genes (*ANGPT1*, *IL1R1*, *TGFB3*, *RASGRF2*, *PAK1*, *MECOM*, *ERBB4*, *KIT*, *NF1*, *MAPKAPK5*, *FGFR4*, *PAK2*, *MAP3K7*, *MAP4K4*), was one of the pathways identified.

Finally, we employed the XPEHH test to analyze the LPB and non-black-bone domestic sheep populations. Based on the empirical distribution (previously 1%), we identified 1193 genes as PSGs (Fig. 2, Supplementary table S11). According to the statistical results, a total of 151 genes have been strongly subjected to selection pressure across the F_{ST} , *LSBL*, and XPEHH methods (Supplementary figure S2). KEGG and GO term analysis of these PSGs revealed that 41 pathways and 2894 terms were significantly overrepresented (Supplementary tables S12 and S13). The MAPK signaling pathway included 28 genes (*TNIK*, *NOTCH2*, *SPAG9*, *PDE6G*, *SLC30A10*, *PTPRC*, *NRP1*, *PLCB1*, *PLCG2*, *FBXW7*, *PTPN11*, *LIF*, *CSPG4*, *EGFR*, *ERBB4*, *PTK2B*, *ADRB3*, *FGFR1*, *INSR*, *FLT4*, *FGFR4*, *ADRA1B*, *ADRA2C*, *KIT*, *FERMT2*, *BMP4*, *TPD52L1*, *SASH1*). A total of 12 genes (*ABCA12*, *CSNK1A1*, *KIT*, *ADAM10*, *RB1*, *CEP131*, *CDH11*, *PEPD*, *PTPN11*, *IFT122*, *TBX10*, and *STAR*) were both detected by F_{ST} , *LSBL*, and XPEHH analysis. These results provide valuable insights into the genetic mechanisms associated with hyperpigmentation in LPB and shed light on

Table 1 Population divergence measured as F_{ST}

Breeds	LPB	LPN	TIB	VLT	OLA	PRT	HUS	CNM	ORI	AGL
Lanping black-boned sheep (LPB)		0.0210	0.0565	0.0797	0.0555	0.0611	0.0718	0.0883	0.1512	0.3006
Lanping normal sheep (LPN)	0.0191		0.0508	0.0739	0.0497	0.0552	0.0647	0.0788	0.1452	0.3038
Tibetan sheep (TIB)	0.0389	0.0372		0.0349	0.0150	0.0184	0.0376	0.0647	0.1283	0.3089
Valley Tibetan sheep (VLT)	0.0584	0.0567	0.0407		0.0404	0.0436	0.0591	0.0840	0.1557	0.3873
Oula sheep (OLA)	0.0426	0.0409	0.0259	0.0491		0.0154	0.0343	0.0622	0.1312	0.3359
Prairie Tibetan sheep (PRT)	0.0494	0.0475	0.0311	0.0552	0.0344		0.0404	0.0689	0.1393	0.3676
Hu sheep (HUS)	0.0512	0.0492	0.0408	0.0610	0.0448	0.0509		0.0549	0.1298	0.3577
Chinese merino sheep (CNM)	0.0488	0.0455	0.0445	0.0596	0.0475	0.0527	0.0485		0.1194	0.3165
Mouflon wild sheep (ORI)	0.0622	0.0586	0.0575	0.0712	0.0594	0.0644	0.0623	0.0539		0.3283
Argali wild sheep (AGL)	0.0845	0.0853	0.0825	0.1079	0.0910	0.0998	0.0988	0.0892	0.0904	

* F_{ST} is given above the diagonal and standard deviation (SD) for each combination is given below.

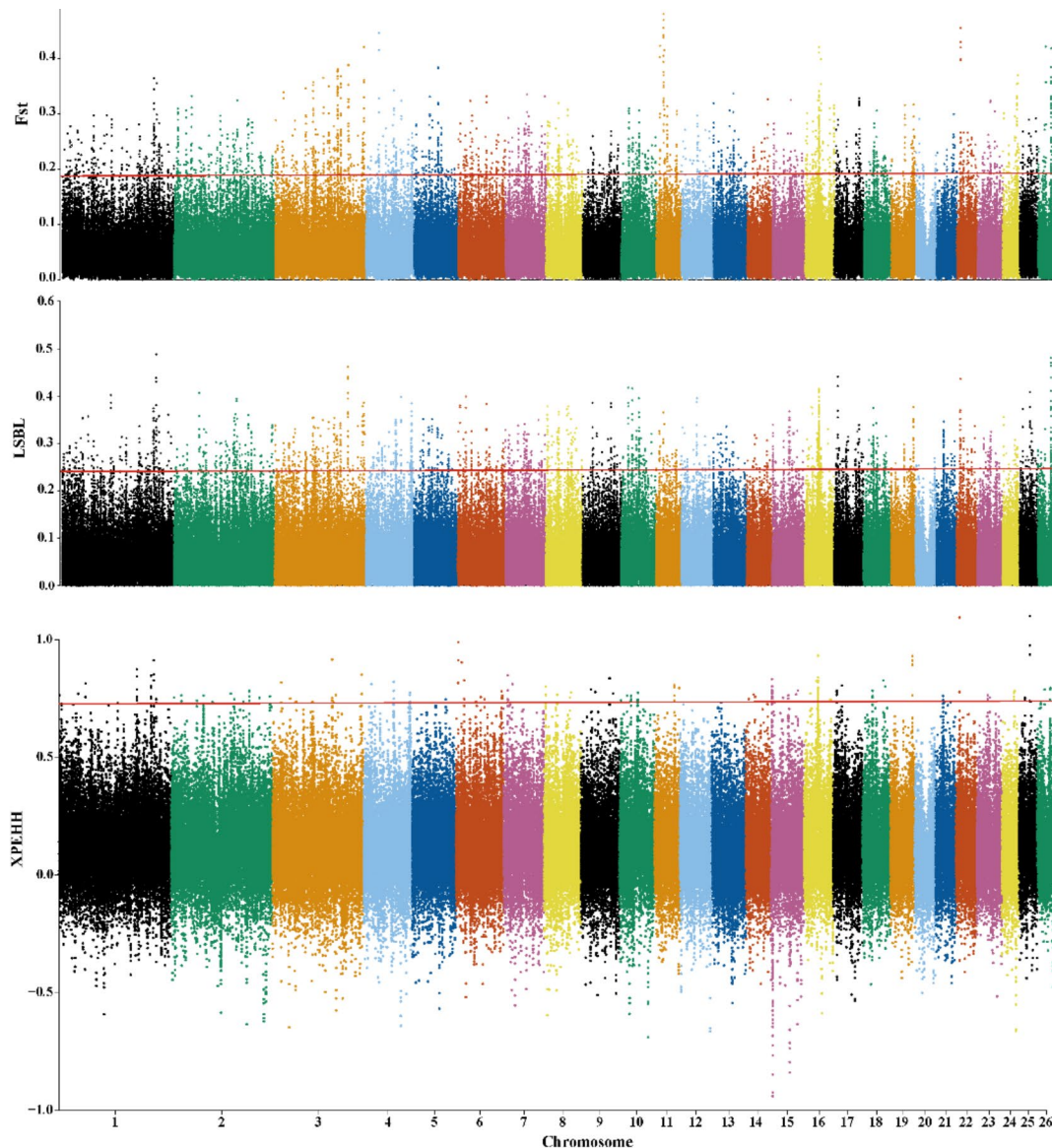


Fig. 2 Genomic regions with strong selective signals (F_{ST} , $LSBL$, and $XPEHH$) in LPB identified by comparing genomes of refined groups of LPB and none black-bone domestic sheep population based on population structure analysis. The population genetic differentiation F_{ST} values, and the $LSBL$ values are were plotted in 20 kb genomic bins with a 10 kb step. The significance threshold of the selection signature was arbitrarily assigned to the top 1% percentile outliers for each individual test and is indicated with red horizontal solid line

the involvement of specific genes and pathways in this unique trait.

DEGs in two pigmentation developmental stages between LPB and LPN

Our previous studies demonstrated that hyperpigmentation in the LPB is the result of ectopic distribution of melanocytes in skin and internal tissues and subsequent melanin synthesized in melanocytes (unpublished data). To understand the differential gene expression associated with pigmentation development in LPB and LPN, RNA-Seq was performed on liver tissues at two different developmental stages: when pigmentation is not yet

visible (2-month-old, stage 1) and when pigmentation becomes evident (2-years-old, stage 2). (Supplementary table S14). Liver tissue was chosen for this analysis due to its high melanin content in adult LPB. The total RNA extracted from sheep liver tissue showed an OD260/OD280 ratio between 1.8 and 2.1, and a total RNA concentration between 0.8 and 3 $\mu\text{g}/\mu\text{L}$ (Supplementary table S15), indicating good purity and concentration of the extracted RNA. Concurrently, the gel electrophoresis results showed that three distinct bands corresponding to 28 S, 18 S, and 5 S rRNA were visible without DNA contamination or RNA degradation bands (Supplementary figure S3), indicating that the extracted RNA had

good integrity. Approximately 1.35 billion raw reads were generated for the analysis (Supplementary table S16).

At stage 1, there were 13,959 and 13,402 expressed genes in the liver tissues of LPB and LPN, respectively. A total of 619 DEGs were identified through comparisons between LPB and LPN (Fig. 3A, Supplementary table S17). Notably, six of these DEGs were enriched in the melanogenesis pathway, with five of them being up-regulated (*PRKACB*, *KIT*, *EDNRB*, *CAM*, and *CAMK*) and one being down-regulated (*Wnt*). (Fig. 3B, Supplementary table S18). Additionally, GO analysis revealed significant enrichment in the molecular function of lipid binding (Supplementary table S19).

At stage 2, there were 13,917 and 13,518 expressed genes in the liver tissues of LPB and LPN, respectively, and 224 DEGs were identified. Among these, 127 DEGs were up-regulated (including 41 exclusively expressed in LPB), and 97 genes were down-regulated in LPB (Fig. 3C, Supplementary table S20). These DEGs were enriched in 18 significantly over-represented KEGG pathways (Fig. 3D, Supplementary table S21), but no pigmentation-related pathways were identified. Over-represented GO clusters were related to the regulation of cellular processes, oxidoreductase activity, and the extracellular region (Supplementary table S22).

Finally, we conducted a further analysis of the interaction between breed and age factors. A total of 35 DEGs were identified, including 7 significantly upregulated genes and 28 significantly downregulated genes ($p < 0.05$) (Fig. 3E, Supplementary table S23). Due to the small number, these DEGs were not significantly enriched in any KEGG pathways. We then performed GO enrichment analysis, which revealed 153 enriched pathways ($p < 0.05$). These pathways were primarily related to immune responses, including innate immune response, defense response to other organisms, response to biotic stimulus, immune response, negative regulation of viral process, and biological processes involved in interspecies interactions between organisms, and no pathways related to melanin were enriched (Supplementary table S24).

Screening of candidate genes related to melanin pathway

To further assess the expression abundance of PSGs identified by F_{ST} and $LSBL$ statistics, the overlapping genes between PSGs and DEGs in two pigmentation developmental stages were investigated. One gene, *KIT*, was found to be shared between PSGs and DEGs. *KIT* is a well-known key gene involved in melanocyte development and melanogenesis. Interestingly, *KIT* exhibited significantly higher F_{ST} and $LSBL$ values, compared to adjacent genomic regions. This suggests a strong selective sweep acting on this gene, indicating its importance in hyperpigmentation. However, the study did not find

significant differences in allele frequencies between LPB and LPN populations (Supplementary figure S4).

To identify candidate genes related to melanin synthesis in LPB, we screened all positive selected genes among four populations (LPB, LPN, none black bone Ovis aries, and wild sheep). Finally, two candidate genes (*ERBB4* and *ROR1*) that may be related to melanin synthesis were identified. Both *ERBB4* and *ROR1* exhibited significantly higher F_{ST} , $LSBL$, and $XPEHH$ values (Fig. 4A), indicating strong selection signals. Among all the positive selection genes screened, only *ERBB4* and *ROR1* showed significant gene frequency differentiation in different populations. Gene frequency analysis revealed that the frequency of mutant alleles was highest in LPB, followed by LPN, and was significantly lower in other populations (none black bone Ovis aries, and wild sheep). Notably, the frequencies of mutant alleles in LPB and LPN were very similar, suggesting a close genetic relationship (Fig. 4B). Even more noteworthy is that these two genes, *ERBB4* and *ROR1*, represent novel findings not previously documented within the list of 688 known melanoma-associated genes [5]. To account for this genetic similarity, the sliding window gene flow analysis was performed, and the results showed that the *ERBB4* and *ROR1* genes were within the window D value range of TOP5%, indicating a relatively large gene flow in the LPB and LPN populations (Dataset S1). This genetic closeness may explain why *ERBB4* and *ROR1* genes were not identified in the transcriptome sequencing results of these two populations.

To eliminate the impact of genetic relatedness on transcriptional results, we further examined two genetically distant populations, LPB and Diqing sheep, using qRT-PCR to detect *ERBB4* and *ROR1* gene relative expression in various tissues. The results demonstrated significant differences in the relative expression levels of *ERBB4* in the spleen and kidney between LPB and Diqing sheep ($p < 0.0001$), with *ROR1* showing similar results in the liver, spleen, and kidney (Fig. 4C), indicating that these genes may play a role in hyperpigmentation in LPB.

Discussion

This study conducted genomic and transcriptomic analyses to explore the genetic basis of hyperpigmentation in LPB. Through genetic structure analysis, we identified both genetic similarities and differences between LPB and LPN, confirming that LPB is a distinct breed derived from LPN. Additionally, the genomic analysis identified several functional genes associated with pigmentation in LPB.

In this study, we performed RNA-Seq analysis to examine the DEGs in liver tissues of LPB and LPN at two distinct developmental stages to elucidate the genetic basis underlying pigmentation development. At the first stage

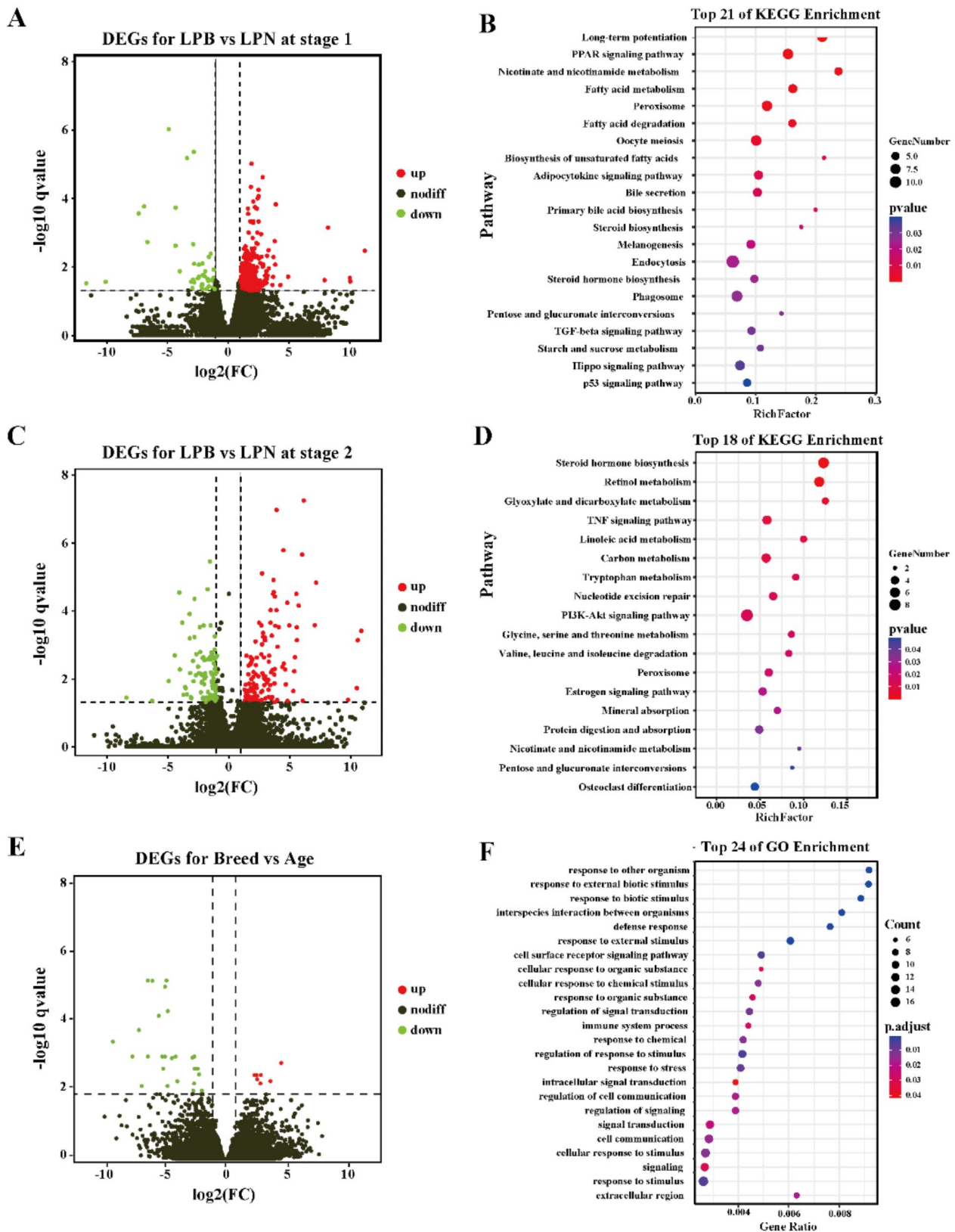


Fig. 3 The volcano plots and KEGG pathways of DEGs between LPB and LPN at stages 1 and 2. **A:** Volcano plot of DEGs identified by comparing the expression levels in liver tissues of LPB and LPN at stage 1. **B:** The significant 21 KEGG pathways of DEGs at stage (1) **C:** Volcano plot of DEGs identified by comparing the expression levels in liver tissues of LPB and LPN at stage (2) **D:** The significant 18 KEGG pathways of DEGs at stage 2. **E:** Volcano plot of DEGs identified by comparing the expression levels in liver tissues of breed vs. age. **F:** The significant 24 GO pathways of DEGs for breed vs. age

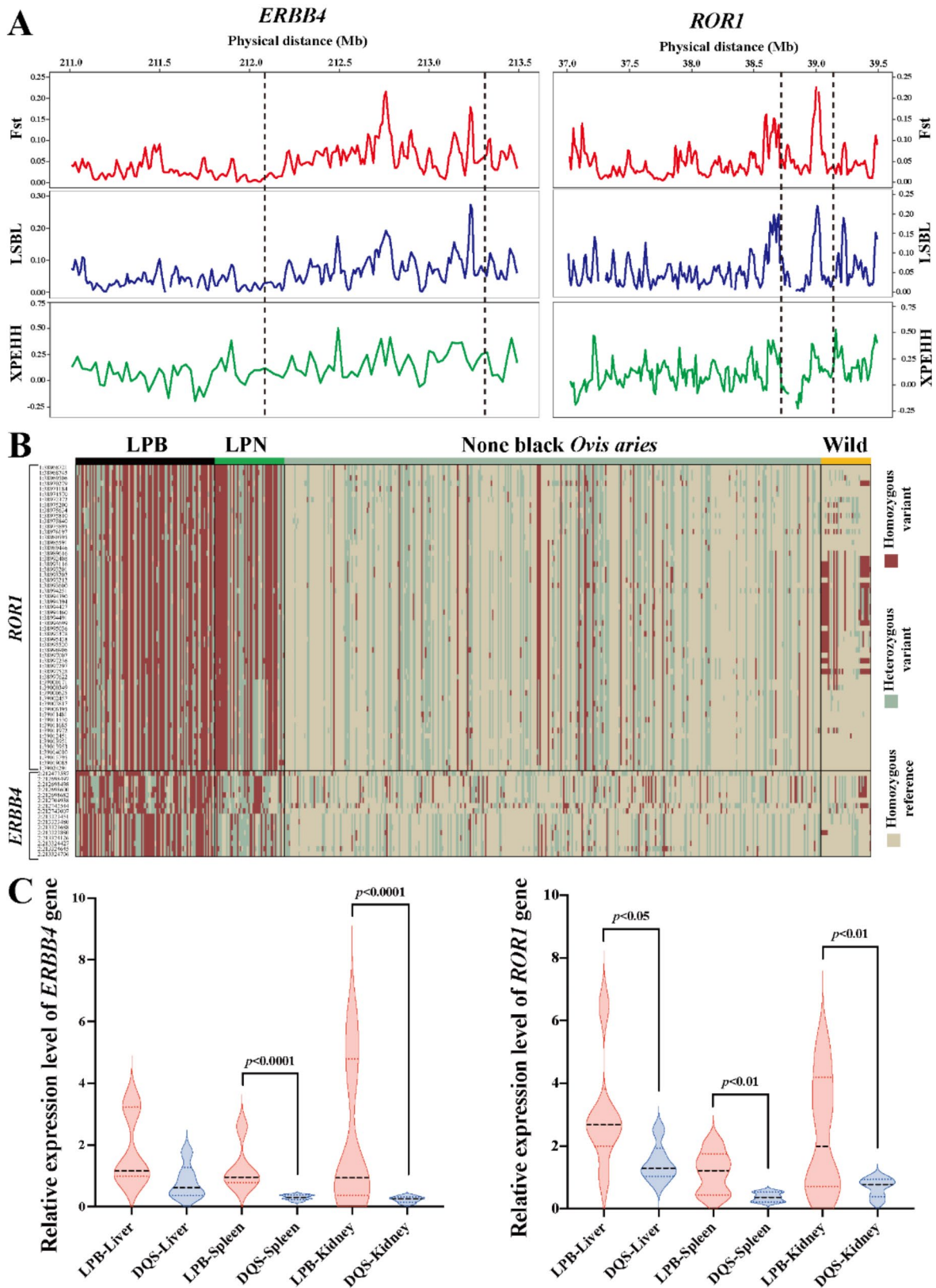


Fig. 4 The relationship between *ERBB4* and *ROR1* genes and hyperpigmentation in sheep. **A:** F_{ST} , $LSBL$, and $XPEHH$ values around the *ERBB4* and *ROR1* genes. The parts within the two black dashed lines correspond to gene positions. **B:** Genotype frequency heatmap of *ERBB4* and *ROR1* genes. **C:** Gene relative expression levels of *ERBB4* and *ROR1* genes in the liver, spleen, and kidneys of Lanping black-boned sheep (LPB) and Diqing sheep. Red represents LPB, blue represents Diqing Sheep

(2-month-old, when pigmentation is not yet visible), five genes (*PRKACB*, *KIT*, *EDNRB*, *CAM*, and *CAMK*) were upregulated, suggesting their potential roles in the early stages of pigmentation. The downregulation of the *Wnt* gene may indicate its inhibitory role in melanogenesis. The significant enrichment in lipid binding functions further implies that these genes may could influence melanin biosynthesis through the regulation of lipid metabolism, offering new insights into the mechanisms underlying early pigmentation in LPB. In contrast, at the second stage (2-years-old, when pigmentation becomes evident), no gene were significantly enriched in pigmentation-related KEGG pathways. This suggests that by this stage, the genetic regulation of pigmentation might have already occurred, or could be governed by factors specific to other tissues. The overrepresented GO terms related to oxidoreductase activity and the regulation of cellular processes imply that the gene expression changes at this stage might be more related to maintaining cellular homeostasis and responding to environmental stressors, rather than directly contributing to melanin production. In summary, our findings highlight the crucial role of gene expression changes, particularly during early developmental stages, in the pigmentation process of LPB.

By combining the selective signature with DEGs, this study identified the *KIT* gene as potentially involved in hyperpigmentation in LPB. The biosynthesis of melanin is meticulously governed by a multifaceted interplay of intracellular signaling cascades, among which the most commonly implicated ones are MC1R/ α -MSH [33], cAMP/PKA [34], MAPK/ERK [35], PI3K/Akt [36], and Wnt/ β -catenin [37] signaling pathway. The *KIT* gene we detected is the member of MAPK signaling pathway. In terms of pigmentation, *KIT* gene mainly regulates the migration of melanocyte precursors to the dermis, epidermis, inner ear, and eye choroid along a specific path [38]. Some studies show that fox white coat was associated with deletion of *KIT* gene Exon 12 [39], white spots in Arabian camels were associated with *KIT* gene mutations [40], the translocation of *KIT* gene led to varying degrees of white spots in cattle [41]. Although the role of *KIT* gene in pigmentation is well-established in other species, no significant frequency differences in alleles were observed between the LPB and LPN populations for this gene. This finding suggests that additional factors may contribute to hyperpigmentation in LPB.

The *ERBB4* and *ROR1* genes were further identified, based on their strong selection signals and significant differences in allele frequencies among four populations: LPB, LPN, none black bone *Ovis aries*, and wild sheep. The *ERBB4* gene encodes human epidermal growth factor 4 (HER-4) and plays a crucial role in cell signaling through autophosphorylation, which, in turn, regulates cell growth and division. Studies have reported that the

expression rate of *ERBB4* protein in melanoma is 66% [42], and the somatic mutation rate of *ERBB4* in metastatic malignant melanoma is 18.99% [43], suggesting that *ERBB4* may play an important role in melanoma. Receptor tyrosine kinase like orphan receptor 1 (*ROR1*) is a member of the *RORs* family that plays a role in the development process, including the growth and development of bones and neurons, cell motility, and cell polarity [44, 45]. *ROR1* is highly expressed in melanoma cells and regulates the phosphorylation of Dvl-2, an upstream component of the Wnt pathway, thereby activating both classical and non-classical Wnt signaling pathways. *ROR1* can positively regulate the expression of Wnt5a, while indirectly activating STAT3 to inhibit the transcription of melanocyte antigens (MART1, GP100, and promoters PAX3 and MITF), leading to decreased pigment proliferation and antigenicity of melanocytes [46]. Furthermore, in melanoma, the *ROR1* gene sustainably undergoes phosphorylation, thus bypassing the Wnt signaling pathway initiated by Wnt5a to promote the occurrence and development of melanoma cells [47], and during the progression of melanoma, *ROR1* can promote tumor cell invasion and metastasis by increasing the expression of *ROR2* [48, 49].

In particular, we found similar allele frequency distributions in both LPB and LPN populations. These two breeds of sheep both live in the same region (Lanping County, Nujiang Prefecture, Yunnan Province, China), and their body shape and appearance are very similar, except for their black traits (such as black eyelids and gums). According to the survey, there is hybridization between the two populations, and our calculated gene flow results for both populations also confirm it, and this provides an explanation for the similarity in gene frequency distribution between those two populations. To mitigate the impact of gene flow, we selected two distant populations (LPB and Diqing sheep), which distributed in Nujiang Prefecture and Diqing Prefecture of Yunnan Province, respectively. Further qRT-PCR detection results showed that in the LPB population, the relative expression levels of *ERBB4* and *ROR1* genes in the liver, spleen, and kidney were significantly higher than those in the Diqing sheep population (except the liver for *ERBB4* gene). The strong selection signals and allele frequency differences among populations suggest that *ERBB4* and *ROR1* could be key regulators of melanin synthesis and contribute to the black traits of LPB.

Conclusion

In conclusion, Lanping black-boned sheep (LPB) represent a valuable model for investigating the genetic mechanisms underlying hyperpigmentation in mammals. Through high-throughput whole-genome sequencing, we generated a vast dataset of single nucleotide

polymorphisms (SNPs) within the LPB genome. The analysis of these autosomal SNPs provides evidence that LPB have evolved as a distinct breed from their none-black-boned counterparts (LPN). Furthermore, we pinpointed two genes, *ERBB4* and *ROR1*, which are potentially associated with melanin synthesis and hyperpigmentation. These findings contribute to a more comprehensive understanding of non-cutaneous melanocyte development and the genetic basis of hyperpigmentation in LPB. The genetic insights obtained from this study not only shed light on the intriguing phenomenon of hyperpigmentation in LPB but also hold broader implications for our understanding of the genetic underpinnings of pigmentation in mammals.

Supplementary Information

The online version contains supplementary material available at <https://doi.org/10.1186/s12864-024-10772-7>.

Supplementary Material 1

Supplementary Material 2

Acknowledgements

We sincerely appreciated that Dr. Yu Jiang from Northwest A&F University and Dr. Dongdong Wu from Kunming Institute of Zoology, Chinese Academy of Sciences freely provided unpublished 421 sheep data and altruistically technical help.

Author contributions

Y.Q.C. the acquisition, analysis, interpretation of data, have drafted the work; H.L.X. the analysis, interpretation of data, have drafted the work; Z.D.G. the analysis; Y.L. the analysis; J.Y.H. have revised the work; J.W. have revised the work; X.M.H. have revised the work; D.M.X. have revised the work; X.L.T. design of the work, analysis, interpretation of data, and have revised the work; W.D.D. the acquisition, interpretation of data, and have revised the work.

Funding

This work was supported by grants from the National Nature Science Foundation of China (32160771, 32302707), Yunnan Provincial Agricultural Union Foundation (202101BD070001-006), Major Science and Technology Projects in Yunnan Province (202202AE090005), Yunnan Province Basic Research Program Project (202301AU070117), Yunnan Provincial Department of Education Science Research Fund Project (2023J0392), "Xingdian Talent" Industry Innovation Talent Program in Yunnan Province (XDYC-CYXC-2022-0029), and Yunnan Provincial Academician and Expert Workstation (202105AF150043).

Data availability

The raw sequences of 150 sheep were deposited NCBI with SRA accession nos. SRR17839521 - SRR18086562. The 23 liver transcriptomic data reported in this article have been deposited in the China National GeneBank DataBase with the project ID PRJCA026513 (BioSample: SAMC3759895-SAMC3759918, <https://download.cnbc.ac.cn/gsa2/CRA016699/>).

Declarations

Consent for publication

Not applicable.

Competing interests

The authors declare no competing interests.

Conflict of interest

The authors declare that they have no known competing financial interests or personal relationships that could have appeared to influence the work reported in this paper.

Ethical approval

All the experimental procedures were approved by the Animal Care and Use Committee of Yunnan Agricultural University (Approval Code: 2022718, Approval Date: 8, July, 2022). The euthanasia process fully complies with local animal welfare laws, guidelines, and policies, and the process is as follows: (1) Anesthesia and Sedation: To minimize pain and distress, all sheep were anesthetized prior to euthanasia. The anesthetic used was xylazine, a common sedative in veterinary practice, and a dosage of 0.5 mg/kg body weight was administered intramuscularly. The dosage was calculated based on the animal's weight to ensure effective sedation. (2) Monitoring Anesthetic Depth: After administering xylazine, the sheep were monitored to ensure they were fully sedated. We checked for signs of deep anesthesia, such as the absence of response to painful stimuli (e.g., pinch reflex), lack of corneal reflex, and muscle relaxation. (3) Euthanasia Procedure: Once deep anesthesia was confirmed, the sheep were euthanized by exsanguination.

Author details

¹Yunnan Provincial Key Laboratory of Animal Nutrition and Feed, Faculty of Animal Science and Technology, Yunnan Agricultural University, Kunming 650201, China

²Yunnan Academy of Animal Husbandry and Veterinary Sciences, Kunming 650224, China

³State Key Laboratory of Genetic Resources and Evolution, Kunming Institute of Zoology, Chinese Academy of Sciences, Kunming 650204, China

⁴Kunming College of Life Science, University of the Chinese Academy of Sciences, Kunming 650204, China

Received: 28 November 2023 / Accepted: 4 September 2024

Published online: 09 September 2024

References

- Dorshorst B, Molin AM, Rubin CJ, Johansson AM, Stromstedt L, Pham MH, Chen CF, Hallbook F, Ashwell C, Andersson L. A complex genomic rearrangement involving the endothelin 3 locus causes dermal hyperpigmentation in the chicken. *PLoS Genet*. 2011;7(12):e1002412.
- Li Y, Zhu X, Yang L, Li J, Lian Z, Li N, Deng X. Expression and network analysis of genes related to melanocyte development in the Silky Fowl and White Leghorn embryos. *Mol Biol Rep*. 2011;38(2):1433–41.
- Shinomiya A, Kayashima Y, Kinoshita K, Mizutani M, Namikawa T, Matsuda Y, Akiyama T. Gene duplication of endothelin 3 is closely correlated with the hyperpigmentation of the internal organs (fibromelanosis) in silky chickens. *Genetics*. 2012;190(2):627–38.
- Deng WD, Yang SL, Huo YQ, Gou X, Shi XW, Mao HM. Physiological and genetic characteristics of black-boned sheep (*Ovis aries*). *Anim Genet*. 2006;37(6):586–8.
- Faraco CD, Vaz SA, Pastor MV, Erickson CA. Hyperpigmentation in the silkie fowl correlates with abnormal migration of fate-restricted melanoblasts and loss of environmental barrier molecules. *Dev Dyn*. 2001;220(3):212–25.
- Saleem MD. Biology of human melanocyte development, Piebaldism, and Waardenburg syndrome. *Pediatr Dermatol*. 2019;36(1):72–84.
- Pillaiyar T, Namasivayam V, Manickam M, Jung SH. Inhibitors of Melanogenesis: an updated review. *J Med Chem*. 2018;61(17):7395–418.
- Yuan XH, Jin ZH. Paracrine regulation of melanogenesis. *Br J Dermatol*. 2018;178(3):632–9.
- Baxter LL, Watkins-Chow DE, Pavan WJ, Loftus SK. A curated gene list for expanding the horizons of pigmentation biology. *Pigment Cell Melanoma Res*. 2019;32(3):348–58.
- Pavan WJ, Sturm RA. The Genetics of Human skin and hair pigmentation. *Annu Rev Genomics Hum Genet*. 2019;20:41–72.
- Dharmayanthi AB, Terai Y, Sulandari S, Zein MS, Akiyama T, Satta Y. The origin and evolution of fibromelanosis in domesticated chickens: genomic comparison of Indonesian Cemani and Chinese silkie breeds. *PLoS ONE*. 2017;12(4):e0173147.

12. Darwish HYA, Zhang Y, Cui K, Yang Z, Han D, Dong X, Mao H, Deng W, Deng X. Molecular cloning and characterization of the endothelin 3 gene in black bone sheep. *J Anim Sci Biotechnol*. 2018;9:57.
13. Han D, Wang S, Hu Y, Zhang Y, Dong X, Yang Z, Wang J, Li J, Deng X. Hyperpigmentation results in aberrant Immune Development in Silky Fowl (*Gallus gallus Domesticus* Brisson). *PLoS ONE*. 2015;10(6):e0125686.
14. Deng WD, Xi DM, Gou X, Yang SL, Shi XW, Mao HM. Pigmentation in Black-boned sheep (*Ovis aries*): association with polymorphism of the tyrosinase gene. *Mol Biol Rep*. 2008;35(3):379–85.
15. Li G, Xiong H, Xi D, Memon S, Deng W. An examination of melanogenic traits and TYRP1 polymorphism in Nanping and Romney Marsh sheep breeds. *Archives Anim Breed*. 2018;61(1):131–41.
16. Deng WD, Tan Y, Wang X, Xi D, He Y, Yang S, Mao H, Gao S. Molecular cloning, sequence characteristics, and polymorphism analyses of the tyrosinase-related protein 2 / DOPACHrome tautomerase gene of black-boned sheep (*Ovis aries*). *Genome*. 2009;52(12):1001–11.
17. Deng WD, Shu W, Yang SL, Shi XW, Mao HM. Pigmentation in Black-boned sheep (*Ovis aries*): association with polymorphism of the MC1R gene. *Mol Biol Rep*. 2009;36(3):431–6.
18. McKenna A, Hanna M, Banks E, Sivachenko A, Cibulskis K, Kernytsky A, Garimella K, Altshuler D, Gabriel S, Daly M, et al. The genome analysis Toolkit: a MapReduce framework for analyzing next-generation DNA sequencing data. *Genome Res*. 2010;20(9):1297–303.
19. Danecek P, Auton A, Abecasis G, Albers CA, Banks E, DePristo MA, Handsaker RE, Lunter G, Marth GT, Sherry ST, et al. The variant call format and VCFtools. *Bioinformatics*. 2011;27(15):2156–8.
20. Wang K, Li M, Hakonarson H. ANNOVAR: functional annotation of genetic variants from high-throughput sequencing data. *Nucleic Acids Res*. 2010;38(16):e164.
21. Yang J, Lee SH, Goddard ME, Visscher PM. GCTA: a tool for genome-wide complex trait analysis. *Am J Hum Genet*. 2011;88(1):76–82.
22. Purcell S, Neale B, Todd-Brown K, Thomas L, Ferreira MAR, Bender D, Maller J, Sklar P, Bakker PIWD, Daly MJ. PLINK: a tool set for whole-genome association and population-based linkage analyses. *Am J Hum Genet*. 2007;81(3):559–75.
23. Retief JD. Phylogenetic analysis using PHYLIP. *Methods Mol Biol*. 2000;132:243–58.
24. Alexander DH, Novembre J, Lange K. Fast model-based estimation of ancestry in unrelated individuals. *Genome Res*. 2009;9:19.
25. Patterson N, Moorjani P, Luo Y, Mallick S, Rohland N, Zhan Y, Genschoreck T, Webster T, Reich D. Ancient admixture in human history. *Genetics*. 2012;192(3):1065–93.
26. Martin SH, Davey JW, Jiggins CD. Evaluating the use of ABBA-BABA statistics to locate introgressed loci. *Mol Biol Evol*. 2015;32(1):244–57.
27. Szpiech ZA, Hernandez RD. Selscan: an efficient multithreaded program to perform EHH-based scans for positive selection. *Mol Biol Evol*. 2014;31(10):2824–7.
28. Raudvere U, Kolberg L, Kuzmin I, Arak T, Adler P, Peterson H, Vilo J. G:profiler: a web server for functional enrichment analysis and conversions of gene lists (2019 update). *Nucleic Acids Res*. 2019;47(W1):W191–8.
29. Zhang DY, Zhang XX, Li FD, Yuan LF, Li XL, Zhang YK, Zhao Y, Zhao LM, Wang JH, Xu D, et al. Whole-genome resequencing reveals molecular imprints of anthropogenic and natural selection in wild and domesticated sheep. *Zool Res*. 2022;43(5):695–705.
30. Kim D, Pertea G, Trapnell C, Pimentel H, Kelley R, Salzberg SL. TopHat2: accurate alignment of transcriptomes in the presence of insertions, deletions and gene fusions. *Genome Biol*. 2013;14(4):R36.
31. Hu XJ, Yang J, Xie XL, Lv FH, Cao YH, Li WR, Liu MJ, Wang YT, Li JQ, Liu YG, et al. The Genome Landscape of Tibetan Sheep reveals adaptive introgression from Argali and the history of early human settlements on the Qinghai-Tibetan Plateau. *Mol Biol Evol*. 2019;36(2):283–303.
32. Yang J, Li WR, Lv FH, He SG, Tian SL, Peng WF, Sun YW, Zhao YX, Tu XL, Zhang M, et al. Whole-genome sequencing of native Sheep provides insights into Rapid adaptations to Extreme environments. *Mol Biol Evol*. 2016;33(10):2576–92.
33. Hsiao JJ, Fisher DE. The roles of microphthalmia-associated transcription factor and pigmentation in melanoma. *Archives Biochem Biophys*. 2014;563:28–34.
34. Bellei B, Maresca V, Flori E, Pitisci A, Larue L, Picardo M. p38 regulates pigmentation via Proteasomal Degradation of Tyrosinase. *J Biol Chem* 2010, 285.
35. Yu-Mi, Kim E-C, Lim LH-M, Young-Kwon. Seo: Rice Bran Ash Mineral Extract increases pigmentation through the p-ERK pathway in zebrafish (*Danio rerio*). *Int J Mol Sci* 2019.
36. Moon H-R, Jo SY, Kim HT, Lee WJ, Won CH, Lee MW, Choi JH, Chang SE. Loratadine, an H1 antihistamine, inhibits melanogenesis in human melanocytes. *BioMed Research International* 2019, 2019.
37. Su T-R, Lin J-J, Tsai C-C, Huang T-K, Yang Z-Y, Wu M-O, Zheng Y-Q, Su C-C, Wu Y-J. Inhibition of melanogenesis by gallic acid: possible involvement of the PI3K/Akt, MEK/ERK and Wnt/ β -catenin signaling pathways in B16F10 cells. *Int J Mol Sci*. 2013;14(10):20443–58.
38. Vandamme N, Bercx G. From neural crest cells to melanocytes: cellular plasticity during development and beyond. *Cell Mol Life Sci*. 2019;76(10):1919–34.
39. Yan SQ, Hou JN, Bai CY, Jiang Y, Zhang XJ, Ren HL, Sun BX, Zhao ZH, Sun JH. A base substitution in the donor site of intron 12 of KIT gene is responsible for the dominant white coat colour of blue fox (*Alopex lagopus*). *Anim Genet*. 2014;45(2):293–6.
40. Holl H, Isaza R, Mohamoud Y, Ahmed A, Almathen F, Youcef C, Gaouar S, Antczak DF, Brooks S. A Frameshift Mutation in KIT is Associated with White spotting in the Arabian Camel. *Genes (Basel)* 2017, 8(3).
41. Hoque MR, Lee SH, Lim DJ, Cho IC, Lee JH. Investigation of KIT gene polymorphisms in Korean cattle. *J Anim Sci Technol* 2012, 54(6).
42. Feinmesser M, Veltman V, Morgenstern S, Tobar A, Gutman H, Kaganovsky E, Tzabari C, Sulkes J, Okon E. Different patterns of expression of the erbB family of receptor tyrosine kinases in common nevi, dysplastic nevi, and primary malignant melanomas: an immunohistochemical study. *Am J Dermatopathol*. 2010;32(7):665–75.
43. Prickett TD, Agrawal NS, Wei X, Yates KE, Lin JC, Wunderlich JR, Cronin JC, Cruz P, Rosenberg SA, Samuels Y. Analysis of the tyrosine kinase in melanoma reveals recurrent mutations in ERBB4. *Nat Genet*. 2009;41(10):1127–32.
44. Green JL, Kuntz SG, Sternberg PW. Ror receptor tyrosine kinases: orphans no more. *Trends Cell Biol*. 2008;18(11):536–44.
45. Valenzuela DM, Stitt TN, DiStefano PS, Rojas E, Mattsson K, Compton DL, Nuñez L, Park JS, Stark JL, Gies DR, et al. Receptor tyrosine kinase specific for the skeletal muscle lineage: expression in embryonic muscle, at the neuromuscular junction, and after injury. *Neuron*. 1995;15(3):573–84.
46. Dissanayake SK, Olkhanud PB, O'Connell MP, Carter A, French AD, Camilli TC, Emeche CD, Hewitt KJ, Rosenthal DT, Leotlela PD, et al. Wnt5A regulates expression of tumor-associated antigens in melanoma via changes in signal transducers and activators of transcription 3 phosphorylation. *Cancer Res*. 2008;68(24):10205–14.
47. Hojjat-Farsangi M, Ghaemimanesht F, Daneshmanesh AH, Bayat AA, Mahmoodian J, Jeedi-Tehrani M, Rabbani H, Mellstedt H. Inhibition of the receptor tyrosine kinase ROR1 by anti-ROR1 monoclonal antibodies and siRNA induced apoptosis of melanoma cells. *PLoS ONE*. 2013;8(4):e61167.
48. O'Connell MP, Marchbank K, Webster MR, Valiga AA, Kaur A, Vultur A, Li L, Herlyn M, Villanueva J, Liu Q, et al. Hypoxia induces phenotypic plasticity and therapy resistance in melanoma via the tyrosine kinase receptors ROR1 and ROR2. *Cancer Discov*. 2013;3(12):1378–93.
49. Matsuda T, Suzuki H, Oishi I, Kani S, Kuroda Y, Komori T, Sasaki A, Watanabe K, Minami Y. The receptor tyrosine kinase Ror2 associates with the melanoma-associated antigen (MAGE) family protein Dlxin-1 and regulates its intracellular distribution. *J Biol Chem*. 2003;278(31):29057–64.

Publisher's note

Springer Nature remains neutral with regard to jurisdictional claims in published maps and institutional affiliations.